ORGANIC LETTERS

2010
Vol. 12, No. 1
12−15

Spirobifluorene-Bridged Donor/Acceptor Dye for Organic Dye-Sensitized Solar Cells

Daniel Heredia, Jose Natera, Miguel Gervaldo, Luis Otero, Fernando Fungo,* Chi-Yen Lin, and Ken-Tsung Wong*

Departamento de Química, Universidad Nacional de Río Cuarto, Agencia Postal 3 (5800), Río Cuarto, Argentina, and Department of Chemistry, National Taiwan University, Taipei 106, Taiwan

ffungo@exa.unrc.edu.ar; kenwong@ntu.edu.tw

Received October 6, 2009

ABSTRACT

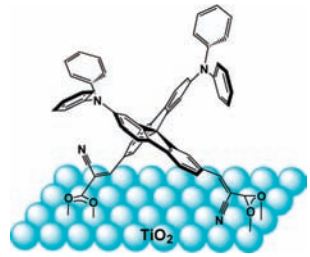

A new dye, SSD1, featuring two donor/acceptor chromophores aligned in a spiro configuration with two anchoring groups separated at a distance of 10.05 Å (closely matching the distance between the adsorption sites of the anatase TiO_2 surface) undergoes efficient dye adherence on TiO_2 films. A dye-sensitized solar cell incorporating SSD1 exhibited a short-circuit current of 8.9 mA cm^{-2}, an open-circuit voltage of 0.63 V, a fill factor of 0.67, and a power conversion efficiency of 3.75%.

The growing worldwide demand for environment friendly energy sources has led to greater interest in solar energy conversion devices. Dye-sensitized solar cells (DSSCs) have been the subject of much research[1] since their report by Regan and Gratzel et al. in 1991.[2] The performance and relatively low production costs render DSSCs as competitive alternatives to conventional silicon-based photovoltaic devices.[3] A crucial issue in DSSC design is the choice of dye used to capture the solar energy. Although many novel structures have been developed and tested as light absorbers in DSSCs, polypyridyl Ru(II) complexes remain dominant in the most successful systems.[4] However, Ru-based dyes are expensive and hard to purify relative to organic sensitizers. Thus, the search for new, highly efficient metal-free dyes remains an active aspect of DSSC development.[3] Organic dyes have many advantageous features, such as the huge diversity of molecular structures available and the possibility of obtaining materials at relatively low cost. Moreover, because organic dyes normally possess higher molar extinction coefficients than Ru dyes (< 20 000 M^{-1} cm^{-1}), they allow thinner nanostructured oxide semiconductor films to be prepared with comparable light-harvesting efficiency—a key factor for practical solid state DSSCs. Another important advantage of organic dyes is that they can be used to construct semitransparent and/or multicolor solar cells, which are potentially useful, for example, in power-producing windows. DSSCs incorporating dyes that are transparent over a region of the visible spectrum would allow part of the visible light to enter a building while simultaneously converting some of the solar power into electricity.

A common strategy in the design of highly efficient organic dyes for DSSCs is the linking of electron donor/

(1) Gunes, S.; Sariciftci, N. S. *Inorg. Chim. Acta* **2008**, *361*, 581.
(2) Regan, B. O.; Grätzel, M. *Nature* **1991**, *353*, 737.
(3) Moreira Gonçalves, L.; de Zea Bermudez, V.; Aguilar Ribeiro, H.; Magalhães Mendes, A. *Energy Environ. Sci.* **2008**, *1*, 655.
(4) Grätzel, M. *J. Photochem. Photobiol. C* **2003**, *4*, 145.

10.1021/ol902314z
Published on Web 12/04/2009

acceptor (DA) systems through conjugated spacers, with TiO_2 surface anchoring groups (e.g., carboxylate) integrated onto the acceptor moiety.[5] Irradiation of these bipolar molecules generates photoinduced intramolecular charge transfer states, which can inject electrons to the TiO_2 conduction band. The preferential orientation of the dye on the surface not only improves charge injection but also maintains the photo-oxidized donor at a distance from the photoinjected electrons, diminishing the impact of deleterious back electron transfer processes. Using this strategy, many bipolar metal-free dyes have been incorporated as efficient sensitizers in DSSCs in recent years.[6−10] Diphenylamine (DPA) and cyanoacrylic acid moieties are among the most commonly employed subunits for the electron donor and electron acceptor/anchoring groups, respectively, in the design of organic dyes for highly efficient DSSCs.[9−14] Variation of the conjugated spacer connecting the donor and acceptor has resulted in dyes reaching remarkable incident photon-to-current efficiencies (IPCEs) and energy conversion efficiencies.[15] The nature of the π-conjugated bridge in the dye influences not only the region of light absorbed by the DSSCs but also the degree of electron injection from the dye's excited state to the TiO_2 surface. A common strategy for efficient harvesting of solar energy is the use of long π-conjugated bridges that red-shift the absorption spectra.[5] The presence of lengthy rodlike structures, however, can lead to aggregation and, therefore, self-quenching and inefficient electron injection into the TiO_2.[13,16] These deleterious processes can be avoided, or suppressed, when the dye molecules possess bulky structural features that impede aggregation.

The bridging of two chromophores perpendicularly via an sp^3-hybridized atom into a spiro configuration allows the constituted π-systems to retain their individual electronic properties (e.g., absorption and emission characteristics). In addition, the high steric demand resulting from the rigid structure efficiently suppresses intermolecular interactions, thereby diminishing the tendency to form aggregates;[17] as a corollary, spiro-configured compounds have higher solubility than their single components. Spiro linkages are particularly beneficial for fluorescent emitters, suppressing the excimer formation that is frequently encountered in the solid state. Molecules possessing a spirobifluorene core and tailor-made optical and redox properties are used widely in organic optoelectronics.[17] For example, 2,2′,7,7′-tetrakis(*N*,*N*-di-*p*-methoxyphenylamino)-9,9′-spirobifluorene (spiro-MeOTAD) is one of the most efficient organic hole transporters used in the development of solid-state DSSC.[18] Nevertheless, it is rare for DSSC dyes to be arranged in a spiro configuration, even though fluorene-containing dyes have been incorporated into DSSCs.[14,19−21] In this study, we synthesized the spirobifluorene-based bipolar dye **SSD1** (Scheme 1) featuring

Scheme 1. Synthesis of SSD1

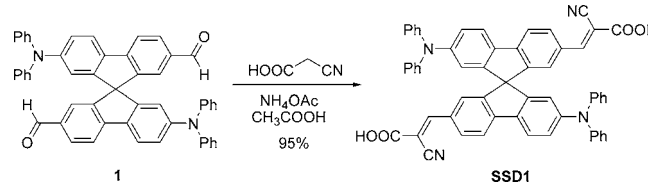

a diphenylamino (DPA) group as the donor and a 2-cyanoacrylic acid unit as the acceptor, with a fluorene bridge ensuring efficient DA interactions. This novel dye possesses several unique features that are potential advantages for application in DSSCs. For example, **SSD1** is composed of two DA branches in a rigid cross-shaped molecular structure, which not only doubles the light absorption efficiency but also minimizes dye aggregation. In addition, two anchoring carboxylate groups are present—one at each electron acceptor site—to improve dye adsorption on basic TiO_2 surfaces and to direct the photoinduced electron injection.[15]

Scheme 1 outlines our synthesis of **SSD1**. 2,2′-Diformyl-7,7′-bisdiphenyamino-9,9′-spirobifluorene (**1**)[22] was reacted with cyanoacetic acid and ammonium acetate in glacial acetic acid at 135 °C for 24 h. The product was purified through reprecipitation from EtOAc and hexane to afford **SSD1** as a red solid in 95% yield.

Figure 1a presents the absorption and emission spectra of **SSD1** in MeCN. We observed two distinct absorption bands: one in the UV region (300 nm), corresponding to the $\pi-\pi^*$ electronic transition of the spirobifluorene core, and the other in the visible region (392 nm; $\varepsilon_{392} = 4.7 \times 10^4\ cm^{-1}\ mol^{-1}$), corresponding to the strong DA intramolecular charge

(5) Kim, C.; Choi, H.; Kim, S.; Baik, C.; Song, K.; Kang, M.-S.; Kang, S.-O.; Ko, J. *J. Org. Chem.* **2008**, *73*, 7072.
(6) Campbell, W. M.; Burrell, A. K.; Officer, D. L.; Jolley, K. W. *Coord. Chem. Rev.* **2004**, *248*, 1363.
(7) Howie, W. H.; Claeyssens, F.; Miura, H.; Peter, L. M. *J. Am. Chem. Soc.* **2008**, *130*, 1367.
(8) Thavas, V.; Renugopalakrishnan, V.; Jose, R.; Ramakrishna, S. *Mater. Sci. Eng. R.* **2009**, *63*, 81.
(9) Mishra, A.; Fischer, M. K. R.; Bäuerle, P. *Angew. Chem., Int. Ed.* **2009**, *48*, 2474.
(10) Chen, Z.; Li, F.; Huang, C. *Curr. Org. Chem.* **2007**, *11*, 1241.
(11) Zhang, F.; Luo, Y.-H.; Song, J.-S.; Guo, X.-Z.; Liu, W.-L.; Ma, C.-P.; Huang, Y.; Ge, M.-F.; Bo, Z.; Meng, Q.-B. *Dyes Pigm.* **2009**, *81*, 224.
(12) Justin-Thomas, K. R.; Hsu, Y.-C.; Lin, J. T.; Lee, K.-M.; Ho, K.-C.; Lai, C.-H.; Cheng, Y.-M.; Chou, P.-T. *Chem. Mater.* **2008**, *20*, 1830.
(13) Ning, Z.; Zhang, Q.; Wu, W.; Pei, H.; Liu, B.; Tian, H. *J. Org. Chem.* **2008**, *73*, 3791.
(14) (a) Baheti, A.; Tyagi, P.; Justin-Thomas, K. R.; Hsu, Y.-C.; Lin, J. T. *J. Phys. Chem. C* **2009**, *113*, 8541. (b) Zhou, G.; Pschirer, N.; Schöneboom, J. C.; Eickemeyer, F.; Baumgarten, M.; Müllen, K. *Chem. Mater.* **2008**, *20*, 1808.
(15) Tian, H.; Yang, X.; Chen, R.; Zhang, R.; Hagfeldt, A.; Sun, L. *J. Phys. Chem. C* **2008**, *112*, 11023.
(16) Ning, Z.; Zhang, Q.; Pei, H.; Luan, J.; Lu, C.; Cui, Y.; Tian, H. *J. Phys. Chem. C* **2009**, *113*, 10307.
(17) Saragi, T. P. I.; Spehr, T.; Siebert, A.; Fuhrmann-Lieker, T.; Salbeck, J. *Chem. Rev.* **2007**, *107*, 1011.
(18) (a) Bach, U.; Lupo, D.; Comte, P.; Moser, J. E.; Weissortel, F.; Salbeck, J.; Spreitzer, H.; Grätzel, M. *Nature* **1998**, *395*, 583. (b) Fabregat-Santiago, F.; Bisquert, J.; Cevey, L.; Chen, P.; Wang, M.; Zakeeruddin, S. M.; Grätzel, M. *J. Am. Chem. Soc.* **2009**, *131*, 558.
(19) Justin-Thomas, K. R.; Lin, J. T.; Hsu, Y.-C.; Ho, K.-C. *Chem. Commun.* **2005**, 4098.
(20) Yen, Y.-S.; Hsu, Y.-C.; Lin, J. T.; Chang, C.-W.; Hsu, C.-P.; Yin, D.-J. *J. Phys. Chem. C* **2008**, *112*, 12557.
(21) Lin, J. T.; Chen, P.-C.; Yen, Y.-S.; Hsu, Y.-C.; Chou, H.-H.; Yeh, M.-C. P. *Org. Lett.* **2009**, *11*, 97.
(22) Chiang, C. L.; Shu, C.-F.; Chen, C.-T. *Org. Lett.* **2005**, *7*, 3717.
(23) Roquet, S.; Cravino, A.; Leriche, P.; Alévêque, O.; Frère, P.; Roncali, J. *J. Am. Chem. Soc.* **2006**, *128*, 3459.

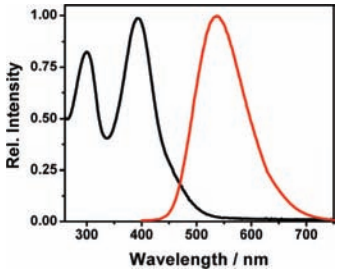

Figure 1. Normalized absorption (black) and emission (red) spectra of **SSD1** in MeCN.

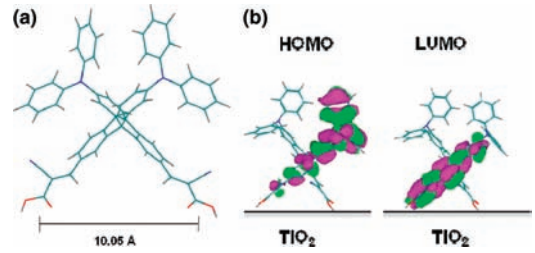

Figure 2. (a) Geometric optimization (AM1) of the structure of **SSD1** and (b) HOMO and LUMO frontier molecular orbitals of **SSD1** obtained from AM1 semiempirical calculations.

transfer (ICT) band,[23] as confirmed by the strong reverse solvatochromism [λ_{max}: 446 nm (toluene), 427 nm (THF), Figure S-1, Supporting Information]. **SSD1** features an emission band centered at 535 nm in MeCN. The absorption spectrum of **SSD1** adsorbed onto fluorine-doped tin oxide (FTO)/TiO_2 nanostructured films; the signals are broader and red-shifted (ca. 30 nm) relative to those in solution (MeCN) (Figure S-2, Supporting Information), presumably because of the interaction between the dye and the nanostructured TiO_2. In addition, the dye exhibits strong absorption in the blue region, giving a film that was light yellow in color. More importantly, a high amount of **SSD1** remained on the electrode surface after several solvent rinses (electrode absorbance was as high as 3.2 after 72 h soaking, and longer soaking time does not change the amount of uploaded dye). We ascribe the high anchoring power of **SSD1** to its two carboxylic groups, which enable the formation of mono- or bidentate binding states with TiO_2.[24,25] The FT-IR spectra (Figure S-3, Supporting Information) reveal that a broadband at 1685 cm^{-1} assigned to the carboxylic acid groups of free **SSD1** completely disappears as **SSD1** absorbed on the TiO_2 surface, providing clear evidence for the double-anchoring behavior of **SSD1**. This result agrees with the observation recently reported by Abbotto et al.[26]

AM1 semiempirical optimization revealed that the distance between the two anchoring acid groups was ca. 10.05 Å (Figure 2a), close to that between adsorption sites on the anatase TiO_2 surface (10.23 Å).[24,25] One important feature of the popular Ru-based dye **N3** is its strong adherence to TiO_2 surfaces through its carboxylic groups, which also allow electronic coupling for electron injection.[15,25] Interestingly, the anchoring groups in **N3** are separated by 10.0 Å.[24] Therefore, it is likely that **SSD1** possesses a suitable structural configuration for efficient surface adherence and subsequent electron transfer. Moreover, the frontier molecular orbitals we obtained through AM1 calculations[27] (Figure 2b) revealed that the highest occupied molecular orbital (HOMO) of **SSD1** is localized mostly on the diphenylamino groups, whereas the lowest unoccupied molecular orbital (LUMO) is localized on the cyanoacrylic acid units. Thus, we anticipated that efficient photoinduced charge separation and the relatively stronger anchoring power would enhance the degree of electron injection to the TiO_2 electrode.

We used cyclic voltammetry (CV) and differential pulse voltammetry (DPV) with Pt as the working electrode to probe the redox properties of **SSD1**. When we scanned the potential between −0.50 and +0.75 V, a reversible redox wave appeared at a value of $E_{1/2}$ of 0.55 V (vs ferrocene/ferrocenium redox couple; equal to 1.10 V vs Normal Hydrogen Electrode (NHE)). We obtained a similar oxidation potential when using DPV (Figure S-4, Supporting Information). Taking into account the optical band gap (2.75 eV) of **SSD1**, we calculated the LUMO energy level to be −1.65 V (vs NHE). The energy levels of TiO_2, **SSD1**, and the I^-/I_3^- redox couple reveal that both electron injection into TiO_2 from the dye's excited states and dye reduction by the I^-/I_3^- couple are exothermic, making DSSC operation feasible (Figure S-5, Supporting Information).

Figure 3 presents the short circuit photocurrent action spectra in terms of the IPCEs[28] of **SSD1**-DSSCs with different absorbances.[29] The IPCE of the resulting photoactive layer shows that **SSD1** adsorbed on TiO_2 successfully extended the photocurrent response into the visible region.

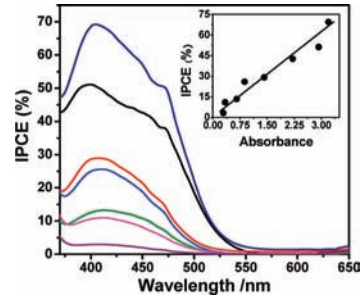

Figure 3. Short circuit photocurrent action spectra (IPCE%) of **SSD1**-containing DSSCs obtained after various soaking times (from a few minutes to 72 h). Inset: change in IPCE% at a wavelength of 405 nm with the electrode absorbance at the same wavelength.

(24) Shklover, V.; Ovchinnikov, Y. E.; Braginsky, L. S.; Zakeeruddin, S. M.; Grätzel, M. *Chem. Mater.* **1998**, *10*, 2533.
(25) Hagfeldt, A.; Grätzel, M. *Acc. Chem. Res.* **2000**, *33*, 269.
(26) Abbotto, A.; Manfredi, N.; Marinzi, C.; De Angelis, F.; Mosconi, E.; Yum, J.-H.; Xianxi, Z.; Nazeeruddin, M. K.; Grätzel, M. *Energy Environ. Sci.* **2009**, *2*, 1094.
(27) Balanay, M. P.; Dipaling, C. V. P.; Lee, S. H.; Kim, D. H.; Lee, K. H. *Sol. Energy Mater. Sol. Cells* **2007**, *91*, 1775.

However, the differences observed between the IPCE and absorption spectrum of TiO_2/**SSD1** indicate the presence of various surface interaction modes, which can affect the charge injection and recombination efficiencies. Interestingly, the IPCE grew continuously as the absorbance increased (inset to Figure 3). The IPCE is given by the equation IPCE $=$ LHE$\varphi_{inj}\eta_c$, where LHE is the light-harvesting efficiency (LHE $= 1 - T = 1 - 10^{-A}$), φ_{inj} is the quantum yield of electron injection, and η_c is the efficiency of collecting the injected electrons at the photoanode. If φ_{inj} and η_c are constant for a given system, the IPCE should reach a plateau at absorbance values greater than one. In this study, however, the relationship between IPCE and absorbance indicates that $\varphi_{inj}\eta_c$ is not constant. Long soaking times allow the TiO_2-coated electrode to accumulate large amounts of **SSD1**; therefore, because of the high value of ε of the **SSD1** dye, the incident light was efficiently extinguished within a thin layer close to the illuminated FTO. Thus, the electrons that were injected from **SSD1** into the nanoporous TiO_2 film had to cross only a short pathway to reach to the FTO, producing a concomitant greater value of η_c.[8] However, with the present evidence, we can not exclude the changes in the injection efficiency along with the amount of dye adsorbed on TiO_2. Nevertheless, the result indicates that even at a high dye concentration, where a close packing of dye on the TiO_2 film exists, there is a low tendency for self-quenching of the dye's excited state through dye aggregation, consistent with steric impediment originating from the spiro configuration.

To compare the performance of **SSD1** relative to that of widely used dye **N3**, we constructed a series of DSSCs featuring thin TiO_2 layers (ca. 1.5 μm) deposited through spin-coating. For both dyes, the electrode absorbances were less than one. We estimated the value of $(\varphi_{inj}\eta_c)_{N3}/(\varphi_{inj}\eta_c)_{SSD1}$ to be 1.12, taken at the maximum absorption wavelength of the electrodes (520 and 418 nm for **N3** and **SSD1**, respectively). This value indicates that the photoinduced electron injection efficiency and electron collection of the DSSCs assembled with **SSD1** were similar to those of devices based on the dye **N3**, which exhibits its very good performance in part because of its ability to keep its positive charge away from the TiO_2 surface, thereby avoiding deleterious back electron transfer.[8] In the case of **SSD1**, the photogenerated positive charge is located on the diphenylamino units, which are positioned at a significant distance from the TiO_2 surface (Figure 2b). In addition, the two carboxylate anchoring groups of **SSD1** not only align with the TiO_2 coordination sites to provide strong bivalent binding but also separate the electrode surface from the photo-oxidized electron donor moieties, diminishing electron/hole recombination. Figure 4 displays the current−voltage curve of the **SSD1** DSSC (TiO_2 film thickness: ca. 7 μm) under AM 1.5 G simulated sunlight.

(28) Vlachopoulos, P.; Liska, P.; Augustynski, J.; Grätzel, M. *J. Am. Chem. Soc.* **1988**, *110*, 1216.

(29) The electrodes were obtained by soaking the TiO_2 films in dye solution, from a few minutes to 72 h, providing surfaces presenting different amounts of adsorbed dye.

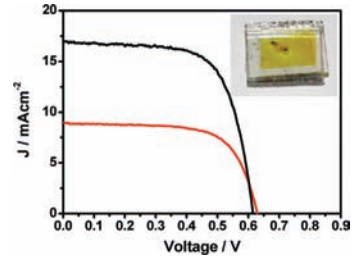

Figure 4. Current−voltage curves for DSSCs incorporating **SSD1** (red) and **N3** (black) under AM 1.5 G simulated sunlight.

The cell exhibits a short-circuit current of 8.9 mA cm^{-2}, an open-circuit voltage of 0.63 V, a fill factor of 0.67, and a power conversion efficiency of 3.75%; for the corresponding **N3** DSSC, these values were 16.5 mA cm^{-2}, 0.61 V, 0.71, and 7.0%, respectively. From the point of view of practical applications, **SSD1** is not panchromatic: only part of the solar spectrum is absorbed. This situation could be rectified, however, through the synthesis of spirobifluorene DA dyes possessing extended π backbones. On the other hand, as the photograph in Figure 4 indicates, the **SSD1** DSSC is yellow, suggesting that it might serve in a semitransparent power-producing window.

In summary, we have synthesized and characterized a spiro-configured DA sensitizer, **SSD1**, for use in DSSCs. The two anchoring groups of **SSD1** are arranged perpendicularly at a distance of ca. 10.05 Å, comparable to that between the two acids in the popular dye **N3** and a close match to the distance between the adsorption sites on the anatase TiO_2 surface (10.23 Å). Strong binding to TiO_2 and suppressed aggregation, due to steric impediment originating from its spiro configuration, make **SSD1** a promising candidate for use in efficient DSSCs. To the best of our knowledge, this paper provides the first example of a DSSC dye based around a DA spirobifluorene structure. We hope that this molecular design triggers further interest in using spiro-configured compounds in DSSCs.

Acknowledgment. We thank Consejo Nacional de Investigaciones Científicas y Técnicas (CONICET-Argentina), Agencia Nacional de Promoción Científica y Tecnológica (ANPCYT-Argentina), Secretaría de Ciencia y Técnica Universidad Nacional de Río Cuarto (SECYT-UNRC), and the National Science Council of Taiwan for financial support. LO, MG, and FF are scientific members of CONICET.

Supporting Information Available: Detailed experimental procedures; spectroscopic characterization, solvent-dependent absorption, cyclic voltammogram, and NMR spectra of **SSD1**; and energy levels alignments. This material is available free of charge via the Internet at http://pubs.acs.org.

OL902314Z